ANALYSIS OF MICRO GAS TURBINE PERFORMANCE USING MODELLING APPROACH

Norazila Othman*

Faculty Of Mechanical Engineering, Universiti Teknologi Malaysia, 81310 UTM Johor Bahru, Johor, Malaysia

*Corresponding email: norazilao@utm.my

Article history
Received
10th September 2023
Revised
24th October 2023
Accepted
25th October 2023
Published
17th June 2023

ABSTRACT

Micro-gas turbine (MGT) is a compact and self-sufficient distributed power generation unit that exhibits reliability and can mitigate carbon monoxide (CO) emissions while conserving energy together with biomass used as a fuel source. It is expected that they will have a noteworthy impact on securing the provision of upcoming energy resources for isolated areas, disaster conditions and off-grid zones regardless of their connection to the power grid. However, the MGT performance using various fuels is still questionable. Databases and procedures of the MGT performance analysis should be established well to understand the overall MGT performance. In this study, MGT performance is determined by utilising computer-aided design (CAD) and solver software such as SolidWorks and Ansys-Fluent. CAD drawing is used to design the combustion chamber and simulation performance is visualised in specific inside the combustion chamber (CC) of the MGT. The solver software was employed to conduct computational fluid dynamics (CFD) analyses. The optimal configuration contained a flame holder with a diameter of 50 millimetres, a chamber height of 60 centimetres, four holes with diameters of 6, 8, and 10 millimetres, and a dead zone separating the combustion and dilution zones. The air inlet boundary conditions were established by utilising the specifications and compressor maps of the Garrett GT25 turbocharger in the simulation. The simulation employed the standard k-ε model of the viscous model and energy equation to establish an optimal maximum airflow rate of 0.15 kg/s at a pressure of 1.4 bar. Three different fuels, diesel-air, wood-volatiles-air, and coal-hv-volatile, were used to determine the MGT's optimal performance. The result shows that wood-volatile-air fuel produces a stable outlet temperature, followed by coal and diesel. Wood has a pressure of 154 kPa and a similar pressure pattern to diesel and coal fuel. Wood gives the maximum exit velocity, while diesel has the lowest. Wood-volatile-air has the lowest mass fraction of fuel at the outlet, while coal-hv-volatile and diesel have equivalent quantities. Diesel-air fuel, which has greater outlet temperatures and velocities, is the most efficient followed by coal and wood. However, wood makes a significant contribution as the alternative fuel replacing the coal and diesel in the MGT chamber as a fuel. The successful investigation of this study opts for a significant contribution to understanding the MGT performance when changing the fuel types giving the awareness to choose one of the alternative power generations which can be used in the future.

Keywords: *Combustion chamber; Computational fluid dynamics; Micro-gas turbine; Power generation; Simulation performance*

1.0 INTRODUCTION

Micro-gas turbines (MGT) are small-scale, independent, and dependable distributed generation systems that have the potential to reduce carbon monoxide (CO) emissions and save energy. It is anticipated that they will play a crucial role in the future energy supply of rural areas with or without grid connections [1]. Micro-gas turbines (MGT) typically generate between 25 to 500 kW of electrical power, have low maintenance and operational costs, a high-density power operation, and low emissions. The ability to function with a variety of fuels is a significant element luring researchers to build MGTs, particularly for renewable energy fuel types. Recent focus has been placed on micro gas turbines for the decentralised generation of renewable energy. A renewed interest in the MGT development and deployment of small-scale distributed cogeneration (DG) and poly-generation technologies has emerged. In addition, MGT engines are becoming increasingly used in the commercial aviation and hobby industries. They are utilised in applications for unmanned aerial vehicles (UAVs) used for missions such as national security, telecommunications, real-time reconnaissance, remote sensing, crime fighting, disaster management, agriculture, and election monitoring [2]. MGTs are also utilised in hybrid electric vehicles, small electricity-generating plants (combined heat and power), and modern aircraft auxiliary power units (APUs). They are appropriate for such applications due to their high density-to-weight ratio, multi-fuel capabilities, and simple design, as well as their low energy costs and emissions. MGTs are a viable and compact alternative to traditional propulsion system power sources, such as battery cells. These engines contain interdependent components with nonlinear properties. Therefore, the entire engine performance is dependent on the performance of each engine piece [3].

Even though the MGT is a great system for the power plant and air transportation, a survey revealed a lack of power plant/engine performance and emission data for the use of biofuel derived from tropical oleaginous plants in micro-turbine engines (Nascimento et al., 2008) [3]. Adapting MGTs to biofuels demands addressing many issues. While natural gas, kerosene, diesel, and even clean biogas can be used directly in micro gas turbines without major modifications, biofuels from the thermo-chemical conversion of biomass or very raw liquid biofuels such as vegetable oil require more extensive redesign and greater modifications to standard technologies before use. In practice, these low-quality renewable fuels employ a series of crucial problems, mostly associated with their unfavorable physical and chemical properties, including low heating value (LHV), high viscosity, poor atomization, and corrosive qualities. Moreover, their chemical-physical properties tend to degrade with storage, and their tar content or deposits might cause fouling on the mechanical moving components (Chiaramonti et al., 2013) [4]. In exploring the MGT performance, the design of a combustion chamber based on temperature homogeneity and CO emission is crucial to make sure this chamber is suitable for use with specific renewable fuels such as wood waste and palm kernel shells. Although conventional design and experimental research on many micro-combustor configurations have been conducted in the past, there is a need for more design and development to address fundamental challenges such as low output temperature and CO emissions (Enagi et al., 2017) [5]. However, there are limited studies on the design of combustion chambers based on biomass fuel as the main source of fuel.

The research carried out by Nascimento et al., (2008) [3] aims to evaluate the thermal performance and emissions of diesel in micro-turbine engines with a capacity of 30 kW that is fueled by diesel, biodiesel, and various blends of the two types of fuel. To evaluate the thermal performance of the 30 kW micro-turbine engine, a cycle simulation was carried out with the help of the Gate Cycle GE Enter software. During the operation, the micro-turbine was put through a series of tests using blends of automotive diesel and castor biodiesel containing 5%, 20%, 30%, 50%, 75%, and 100% biodiesel, respectively. A 30-kW diesel micro-turbine engine that was installed was put through its paces in terms

of performance and emissions testing, and the results of the performance tests were compared to those of the simulation. The results are described in Figure 1(a) [6-8].

Extensive research has shown that in the power range from 12 kW to full load, the values derived from numerical modelling and actual testing are extremely similar, as shown in Figure 1(a) tested in a micro gas turbine. For loads less than 12 kW, simulated figures and experimental test values varied significantly. The percentage discrepancy between the simulated values and the experimental results at a power of 12 kW was around 4.7% for BD50 and 7.7% for BD100. Figure 1(b) compares the volumetric fuel flow of the numerical simulation and the experimental testing concerning the power for BD50 and BD100 blends. Comparing the findings obtained with diesel to those obtained with biodiesel and its mixes, no significant difference in the micro-turbine heat rate was noticed during the experimental test. According to the results of the thermal performance tests, the specific consumption of pure biodiesel was greater than that of diesel. The reason for this is that the heat value of pure biodiesel is significantly lower in comparison to the heat value of diesel. During the thermal performance testing, the operation of the 30 kW micro-turbine diesel engine did not alter in any way, nor were any vibrations, sounds, operating failures, or difficulties in starting the engine observed [4-5].

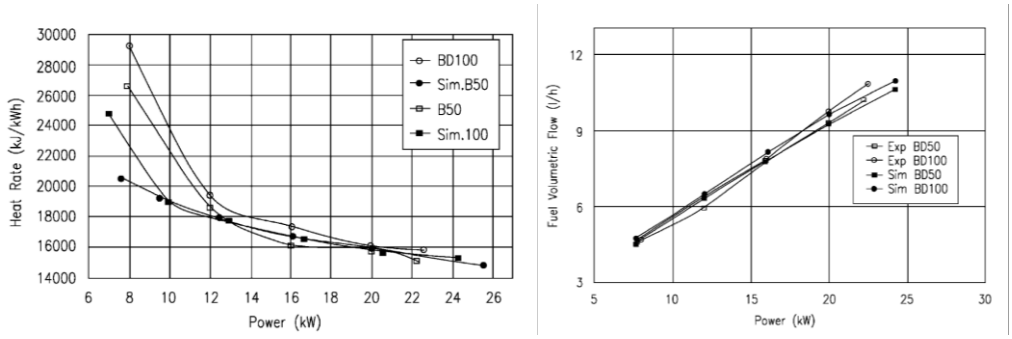

(a) (b)

Figure 1: (a) Absolute heat rate at partial loads for diesel, biodiesel and their blends for tests and simulation results, **(b)** Fuel volumetric flow versus corrected power output for diesel, biodiesel and their blends for tests and simulation results.

As shown in Figure 1, an investigation of the power output using biodiesel blends is important in MGT. Thus, when changing the fuel for example from diesel to wood, it is necessary to study the MGT performance affected by fuel. In this study, the determination of the MGT performance is performed using the selected biomass waste such as coal and wood instead of diesel fuel to investigate the combustor capability with wood. In addition, the numerical analysis for the new combustor design is important before the experimental task takes place to give logical information in the design phase and reduce the experimental cost for research and development activities. Moreover, this study determines the effect of parameters such as temperature, pressure, burning velocity and mass fraction during operation in the combustion chamber is investigated numerically. Utilising different types of fuel in simulation is covered to establish the performance effect of the designed combustor on the change of the fuel. The modelling of the MGT for the combustion chamber using commercial computer-aided design (CAD) software, SolidWorks, and commercial solver, Fluent for numerical and simulation analysis.

2.0 MODELING AND SETUP

In this study, the investigation of the MGT performance focuses on chamber design analysis numerically. The first task was performing the chamber design schematic diagram, the second task was performing the mesh generation for the chamber modelling, pre-

processing set up for the solver, running the simulation, post-processing the result and visualization. For chamber design, a criterion for selecting suitable combustor geometry was carefully examined followed by a designed calculation of the dimensions specifically. The combustion chamber design is faced with inherent challenges such as emission control, chamber materials temperature limitations and flame stability. The steps taken in designing the chamber are using computer-aided drawing software SolidWorks, and simulation using Ansys-Fluent software [1,3,6]. The modelling and setup framework are described in detail in the subsection below such as chamber configuration design, governing equation involved in this study, and simulation setup [7-10].

2.1 Chamber Design and Configuration

The combustion chamber consists of the air jacket and flame tube with a 100 mm fixed height conical exit of the chamber. Chamber inlet and outlet diameters were also fixed at 50 mm diameter to match the specifications of the first stage MGT Garrett GT25 [5] as shown in Figure 2.

The best design of the combustion chamber in this study was the utilisation of stainless steel (SS) pipelines with a thickness of 6 mm for the outer air jacket and flame tube, while a 10 mm thick SS plate was employed for the top plate as shown in Figure 3. The chamber geometry that yields the best results is characterised by a height of 600 mm, an inner diameter of 152 mm, and an orifice height of 100 mm at the exit. The design of the flame container utilised a flame tube configuration, featuring a vertical height of 690 mm and an internal diameter measuring 50 mm. The combustion zones were comprised of four rows consisting of eight holes each. The largest dead zone, which spanned between the primary and dilution zones, had a width of 350 mm. The respective dimensions of the holes in the zones designated for premixing, primary, and dilution were 6 mm, 8 mm, and 10 mm.

The main manipulated geometries in the range were chamber height, chamber diameter, flame tube diameter and combustion zone configurations on the flame tube. Flame tube diameter was varied in the range of 50–150 mm, thus, chamber diameter was varied accordingly to leave air jacket space of 25 mm, while chamber height was varied from 300 to 1000 mm. Simple flame tube geometry with fixed rows of holes of 6 mm diameter through the tube height was studied first. However, for the final flame tube optimization, three zones were identified on the flame tube: premix zone, primary combustion zone and dilution or cooling zone. Each zone has several rows with a certain number of holes on each row with space between zones. The number of rows varied from 4 to 15 for each zone and some holes in each row also varied from 4 to 10. Two holes diameters arrangements respective to the zones were studied: 6, 8, 10 mm and 8, 10, 12 mm. To simplify the meshing and simulation processes, the flame tube was built as a void inside the chamber instead of a solid body. This was achieved by creating two separate bodies (chamber and flame tube) and then subtracting the flame tube body from the chamber. Figure 4 shows the rendering modelling of the MGT in the current study.

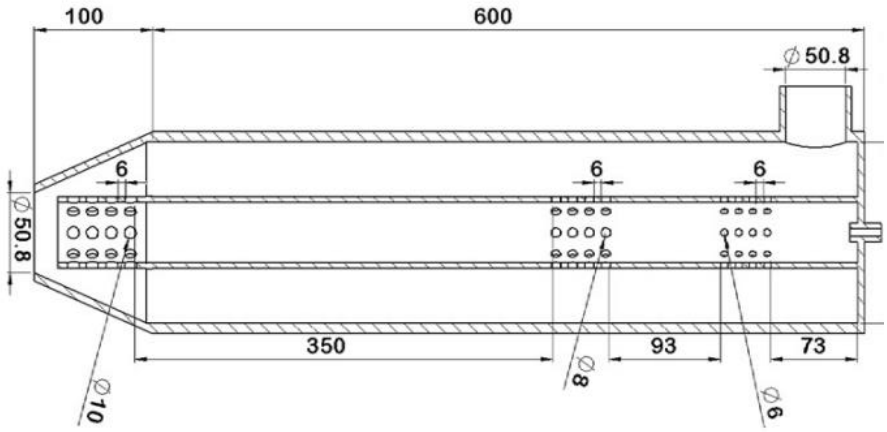

Figure 2: Combustion chamber drawing based on the MGT GarrettGT25 [5].

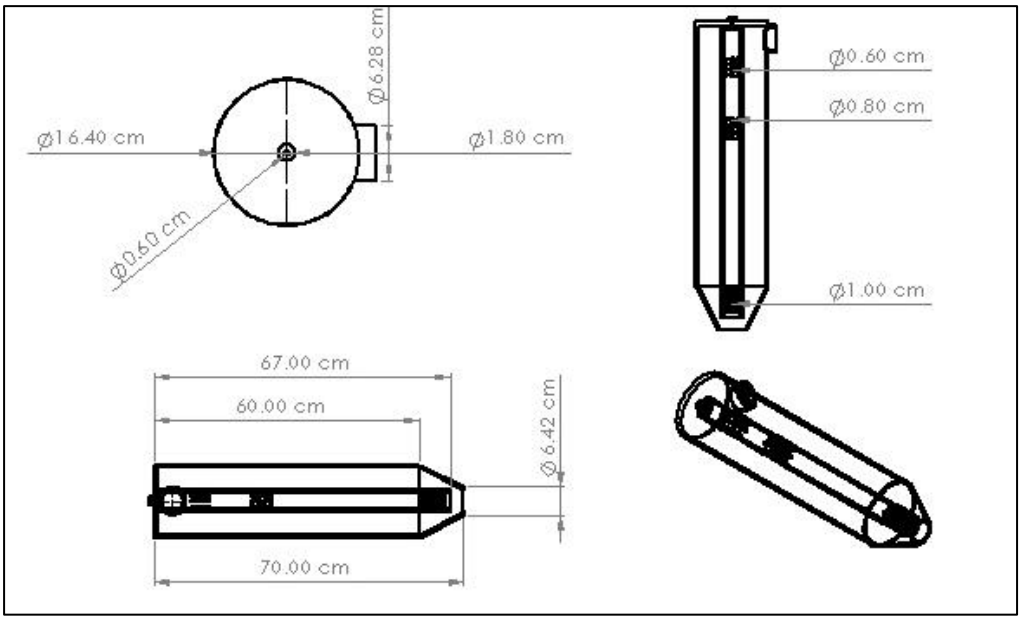

Figure 3: Orthographic view of the MGT in the current study.

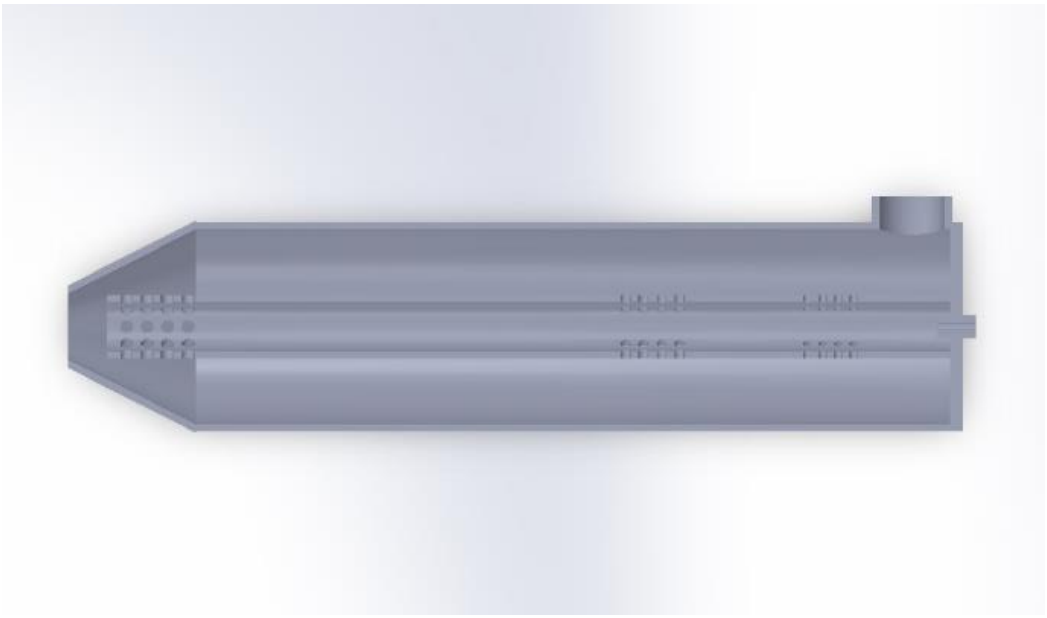

Figure 4: Combustion chamber drawing in the current study.

2.2 Meshing Generation

The next task for the modelling before the simulation was preparing the meshing generation for the combustion chamber model. In general, for any numerical and simulation study the cell topology is essential to the process of meshing. It is essential to first keep in mind that Ansys meshing can produce both 2D and 3D meshes, in contrast to Fluent meshing, which is only capable of producing 3D meshes. Both tools have the capability of generating meshes in 3D that contain tetrahedral, hexahedral, prism/wedge, and pyramid parts. The Mosaic Meshing technology offered by Fluent differentiates itself from similar offerings by making use of conformal polyhedron pieces. Polyhedral has several advantages over tests, including a significantly lower cell count, improved gradient calculations due to the increased number of faces, and the ability to easily represent complex geometries while maintaining their simplicity. The element size used in this study was 3mm as default and the maximum adaptive size was 6mm. For the curvature minimum size was set at 0.03mm and the curvature angle was 18°. In addition, the bounding box diagonal was approximated at 0.73m, the average surface area was 0.00005mm^2 and the minimum edge length was 0.0188mm. The total numbers of faces and edges were 108 and 203, respectively. The orthogonal quality of the mesh sizes for the combustion chamber was determined to be 0.77. A total of 1,438,357 mesh cells were generated, resulting in a total of 2,058,795 nodes. It is recommended to have a minimum orthogonal quality of 0.05 or higher. Figure 5 and Figure 6 are the details of the grid models.

The selection of meshing face elements or cell sizes was determined by considering factors such as proximity and curvature. The mesh sizing function, as depicted in Figure 7 specifies the meshing operation data set-up and other relevant parameters. These settings aim to ensure the appropriate orthogonal quality of mesh sizes for subsequent. After establishing the mesh measurement data, modifications were made to ascertain the overall dimension of the mesh and orthogonal quality.

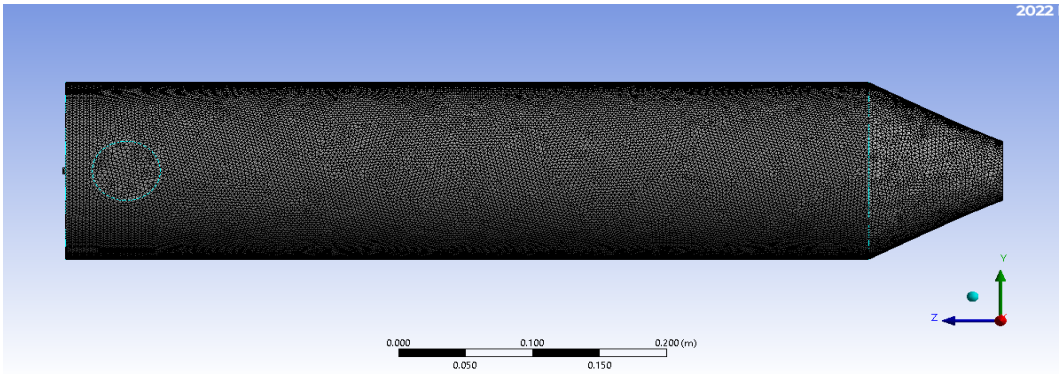

Figure 5: Side view of mesh grid model

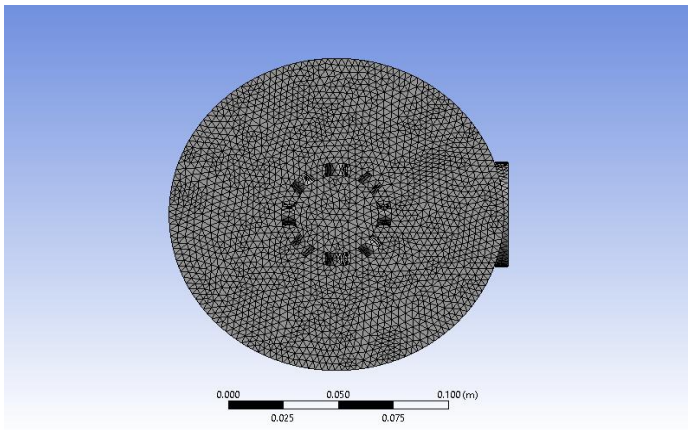

Figure 6: Front view of mesh grid model

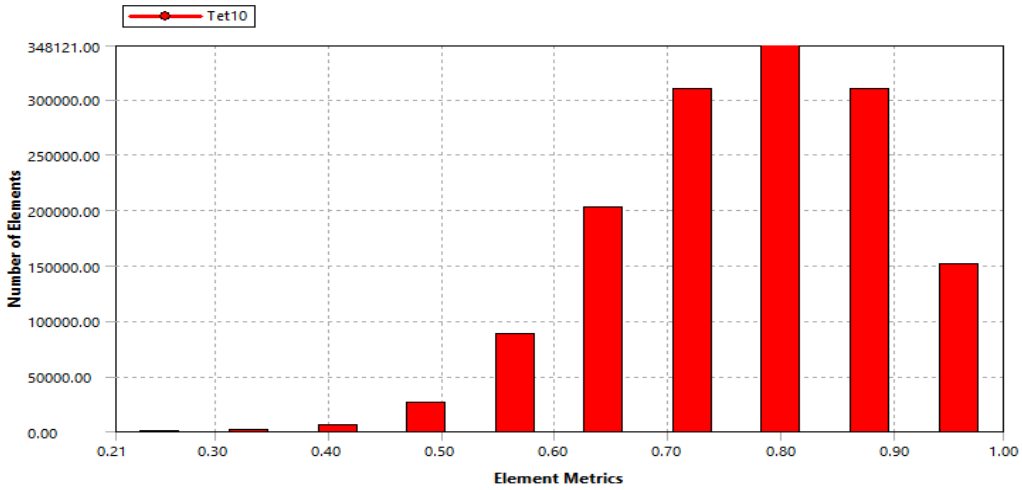

Figure 7: Bar chart of orthogonal quality.

The grid independence test was used in this study by checking the results for two consecutive cell sizes that are identical, indicating that the grid can be considered independent. The ANSYS FLUENT solution employed to assess mesh sensitivity involved comparing two distinct cell sizes based on the total temperature magnitude. In the first phase, a grid size of 0.003m was employed, resulting in the generation of 1,438,357 cells. In the second phase, a mesh size of 0.004m was employed, resulting in the generation of 725,271 cells. Using the ANSYS FLUENT surface integration method, the average temperature for Phases 1 and 2 was calculated. Phase 1 had an average temperature magnitude of 1172.804 K, while Phase 2 had an average temperature magnitude of 1151.54

K. This indicates that the difference between the two phases is only 1.81 per cent. To assure precise outcomes within the computer's computational limitations, a uniform grid size of 0.003 m was used to simulate all models in this study.

2.3 Boundary Conditions Setting

The air inlet boundary conditions were determined based on the specifications and compressor maps provided by the Garrett GT25 turbocharger [5]. A compressor efficiency of approximately 70% was found to be attainable by maintaining an optimal maximum airflow rate of 0.15 kg/s at a pressure of 1.4 bar. The optimal chamber design should aim to achieve efficient combustion with minimal carbon monoxide (CO) emissions and consistent flame propagation within the flame tube, while also maintaining a compact structural configuration. Table 3.1 displays the primary boundary conditions of the air and fuel inlets, chamber outlets, and walls (Enagi et al., 2017) [5]. Table 1 shows the parameters set for the boundary conditions.

Table 1: Parameters set out in boundary conditions.

Parameters	Value
Fuel Inlet	
Temperature	300 K
Pressure	2 bars
Mass flow rate (Diesel) (20% excess air)	0.0056 kg/s
Air Inlet	
Temperature	530K
Pressure	1.4 bar
Mass flow rate	0.15 kg/s
Outlet	
Pressure	1.4 bar
Back flow temperature	600 K
Inner walls	
Materials	Steel
Emissivity	0.5
Outer walls	
Materials	Steel
Wall thickness	6 mm
Heat fluxes	-10,800 W/m^2

2.4 Simulation Setup

Combustion chamber geometry was optimized using the Ansys 2022 R1 CFD simulations program. In the Workbench, chamber geometry was imported from SolidWorks to the Design-Modeler tool. The meshing (Ansys ICEMCFD) tool was used to create the mesh and test its quality. After that, a 3D simulation was performed on the mesh using the Fluent CFD tool. The air inlet boundary conditions were established using the specifications and compressor maps of the Garrett GT25 turbocharger [5]. An ideal maximum airflow rate of 0.15 kg/s at 1.4 bar was determined to achieve a compressor efficiency of around 70%. The ideal chamber must achieve efficient combustion with minimal CO emissions and consistent flame propagation in the flame tube, all while retaining a compact structure. Table 1 presents the main boundary conditions for the air and fuel inlets, chamber outlets, and walls.

The setting for the viscous model is using the standard k-ε two equations model with the model constant of 1.9 C2-epsilon constant, and 0.85 for energy Prandtl numbers and wall Prandtl numbers, respectively. In the present study, the working fluid utilized in

the project was identified as air. The species transport was used for a mixture of material import from the CHEMKIN mechanism database. The mixture selected is diesel air from the fluent library as the conventional fuel and air. The reaction is set to volumetric due to volumetric reactions are crucial to understanding the behaviour of materials and structures under different conditions and are commonly encountered in various engineering disciplines, including structural analysis, fluid mechanics, and heat transfer.

An eddy-dissipation model (EDM) [11] is chosen as the turbulence-chemistry reaction, it is turbulence-chemistry reaction refers to a modelling approach used to simulate the interaction between turbulence and chemical reactions. The interplay between turbulence and chemical reactions in combustion systems is of the utmost significance in determining various aspects such as combustion characteristics, pollutant formation, and heat release. The eddy-dissipation model aims to capture this interaction by considering the influence of turbulence on the rate of chemical reactions. This model assumes that the fuel and oxidizer are carried by separate eddies in diffusion flames with finite-rate chemistry for solving supersonic turbulent combustion. In addition, turbulent eddies are known as fine structures where the actual dissipation of turbulent kinetic energy into heat and simultaneous mixing occurs in fine scales and occupy a very small fraction of actual fluid volume. The scheme used in the solution method is coupled which refers to the solution method used to solve the governing equations for fluid flow, heat transfer, and other related phenomena. The solution controls have been determined and the normal solution setup was 0.5 for pressure factor and momentum respectively, 0.25 for density factor and 0.75 for turbulent kinetic energy and turbulent dissipation rate. Consequently, the problem-solving process involved the computation of data obtained from the model's inlet. The iterative processes were carried out consecutively, with a total of 300 iterations. This choice was made because a higher number of iterations is likely to yield more accurate results before reaching convergence.

Figure 8 depicts a scaled residual plot to demonstrate the convergence of solutions across the simulations carried out in this study. Converged solutions can be obtained through iterative solution processes, in which the solution is considered converged when all discretized transport equations meet the specified tolerance defined by residuals, or when the outcome no longer changes significantly with the following iterations. However, the accuracy of convergence may be compromised if it does not align with any corresponding simulation data. Furthermore, the parameters governing the convergence of the solution are explicitly defined within the residual monitors. The scaled residuals may be graphed alongside the iterations computation until the solution achieves convergence. It was noted that there was minimal variability in the residuals as the number of iterations approached 300.

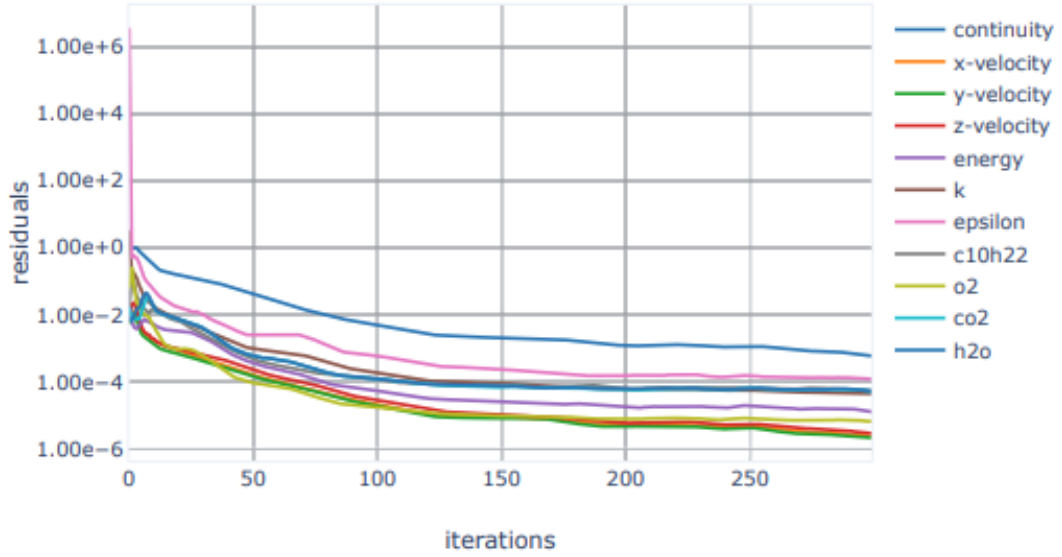

Figure 8: Scaled residuals plot with solution convergence.

2.5 Governing Equation

For any combustion activities in the combustion chamber, the reactant and product mixtures can be declared as the stoichiometric quantity of oxidizer needed to completely burn a quantity of fuel. For a hydrocarbon fuel given by C_xH_y the stoichiometric relation can be expressed as Equation (1) for the reactant (oxygen and nitrogen) and product of the mixtures (carbon dioxide, water, and nitrogen) for the complete combustion. Thus, the stoichiometric air-fuel ratio (*AFR*) is the ratio of air to fuel within a combustion mixture utilized by combustion activities. This parameter denotes the volumetric flow rate of air and fuel that is being delivered to the cylinders of the engine during the combustion process. The utilization of lean mixtures has the potential to enhance fuel efficiency. However, they also increase the risk of engine misfires and can result in higher combustion temperatures, which can potentially damage engine components such as chambers, valves, compressors, and turbines. In general, the *AFR* formula is shown in Equation (2).

$$C_xH_y + a(O_2 + 3.76N_2) \rightarrow xCO_2 + (y/2)H_2O + 3.76aN_2 \quad (1)$$

Where; $a = x + y/4$

$$AFR = \left(\frac{m_{air}}{m_{fuel}}\right)_{stoic} = 4.76a\left(\frac{MW_{air}}{MW_{fuel}}\right) \quad (2)$$

Where;

AFR is the air-to-fuel ratio.
MW_{Air} are the molecular weights of the air.
MW_{fuel} are the molecular weights of the fuel.

3.0 RESULTS AND DISCUSSION

In this study, assessing the most efficient operation of a Micro Gas Turbine (MGT), was for three distinct fuel types were employed: diesel-air, wood-volatile-air, and coal-hv-volatile revealing the optimal performance of the MGT with the designed combustion

chamber. The findings provide valuable insights into fuel selection for maximizing the efficiency and effectiveness of MGT operations.

3.1 Computational Analysis Verification

The initiative for the start of the verification is compared with the computational result by Enagi et al., (2017) [5] with this study for the desired temperature data is obtained. This information is crucial for accurately reproducing the simulation. Figure 8 shows the comparison of the visualization temperature contour from Enagi et al. (2017) [5] and the current simulation yielded in this study using diesel fuel as conventional fuel. Comparison based on the outflow temperatures of 2050 K and 2062 K, respectively. The percentage difference is 0.58% acceptable for the current study when compared with Enagi et. al (2017). The temperature contour from Figures 9(a) and 9(b) Enagi et al. (2017) is depicted in Figure 9.

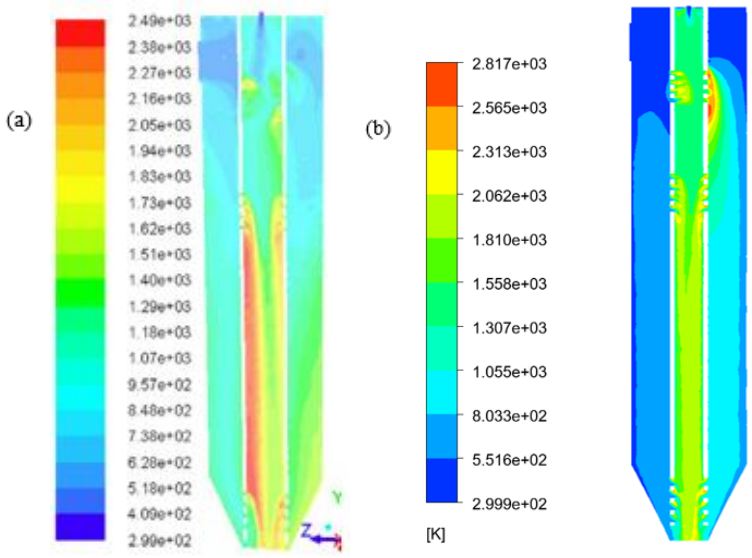

Figure 9: Temperature contour from (a) current study and (b) Enagi et. al. 2017

3.2 Parameters Distribution at the Middle Line

This analysis involves a review and comparison of the central region of the combustion chamber across three distinct fuel types, namely diesel, wood, and coal. The setup of the midline involves the utilisation of the line option and the setting of its position along the *z*-axis, with the distances along the *y* and *z*-axes being both set to zero. Figure 10 shows that combustion raises wood-volatile-air and coal-hv-volatile temperatures above 1800 K. However, for diesel-air fuel combustion hits 1354.69 K and stagnates before reaching 1800 K at 0.1 m. Based on outlet data, diesel-air fuel combustion produces the greatest temperature of 2151.56 K, whereas wood-volatile-air combustion produces 1876.99 K and 2061.24 K, respectively [12-14]. The wood-volatile-air records a stable temperature compared to the coal-hv-volatile and diesel-air fuel. The low temperature in the chamber causes the lower performance of combustion from wood-volatile-air fuel source. Practically, using diesel and coal as a fuel, the complete combustion is happened due to the high temperature gained from these two fuel sources compared to wood.

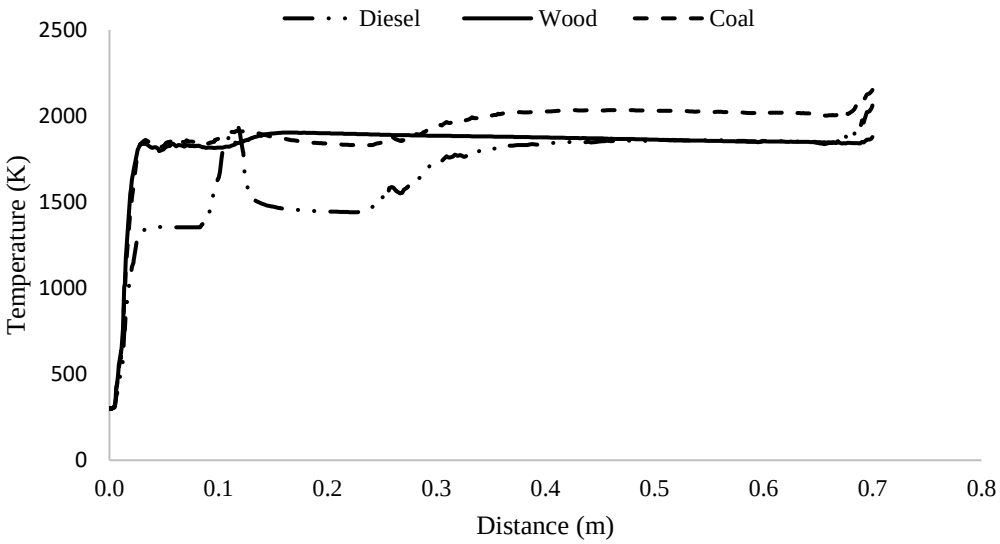

Figure 10: Temperature distribution at the middle line

Figure 11 shows that diesel-air, wood-volatile-air and coal-hv-volatile pressures decline slightly after ignition and stay constant until 0.65 metres. At this point, the pressure levels of wood species experience a drop to 141855 Pa even though the initial pressure exerted by wood-volatiles-air is recorded to be greater than 160000 Pa, which then decreases dramatically at 0.02 metre. Nevertheless, the pressure then experiences an increase and reaches 152965.84 Pa at 0.1 meter. Multiple factors can lower pressure during combustion such as burning fuel produces high-pressure gases when using wood, gases from the combustion chamber expand and displace the surroundings, thus lowering the pressure [15-19]. In addition, for the diesel and coal the pressure maintains until 0.65 m approximate at 154000 Pa. The thermochemical properties for the diesel and coal prove that the suitability of these two-fuel source as the fuel for the conventional engine, but the wood still acceptable as the alternative fuel source in MGT.

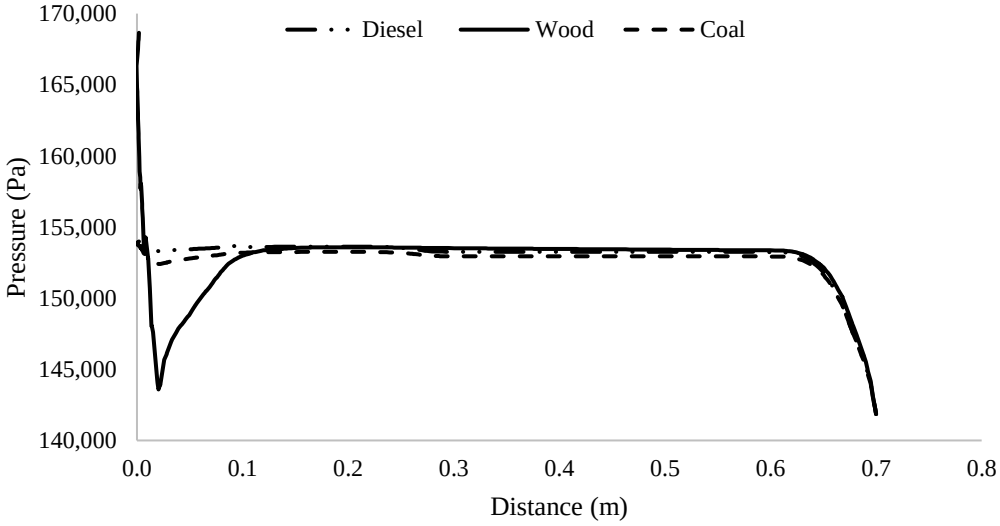

Figure 11: Pressure distribution at the middle line.

According to the data presented in Figure 12, the burning velocity is the speed at which a flame front propagates relative to the unburned gas. It is an essential parameter for the safe design of equipment and processes. According to Figure 12, the maximum burning velocity

attained after ignition is associated with wood-volatile-air fuel, with a recorded value of 508.2 m/s. The higher velocity using wood means high relative to the unburned gas that happens inside the chamber, far from complete combustion and low temperature [15-16]. At 0.159 m, the burning velocity decreased to 128.55 m/s and remained constant until it increased again at 0.6 m. The burning velocity was measured to be 353.42 m/s. The velocities of diesel-air and coal-hv-volatile following ignition are 52.11 m/s and 163.06 m/s, respectively. Less velocity for both fuels' diesel and coal because less relative to the unburned gas and complete combustion with high temperature. In addition, both burning velocities have a comparable pattern, characterised by a decrease at 0.2 metres, followed by an increase before reaching a steady burning velocity at 0.3 m. The burning velocities for diesel-air and coal-hv-volatile are 327.78 m/s and 374.41 m/s, respectively. For the chamber design, the high burning speed causes a longer design for the chamber configuration and vice versa. Besides that, using wood, the flammability limits are low, the oxygen concentration is high, and the gas deflagration index is low. The variations in burning velocity observed among distinct fuels after ignition can be assigned to their diverse energy content, stoichiometric ratios, chemical compositions, and combustion efficiency [17-21].

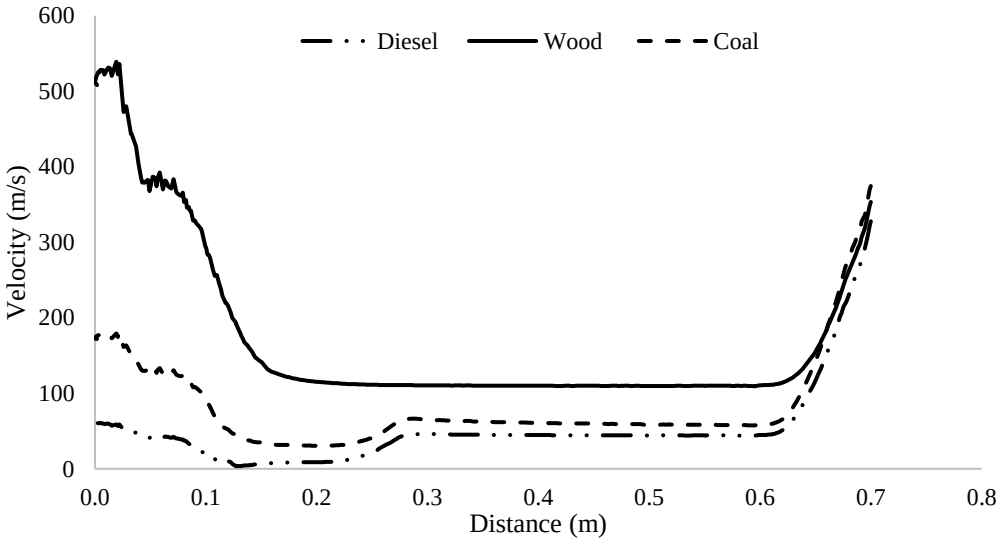

Figure 12: Velocity distribution at middle line

According to the data presented in Figure 13, the mass fraction of wood experiences a decrease to 0.6 after ignition, and afterwards undergoes a further reduction of 0.43 at 0.2 meters. The mass fraction of diesel and coal exhibits a comparable pattern after ignition. The sudden fluctuation in diesel fuel levels occurring at 0.1 m may be attributed to the turbulence of air coming from the primary zone. Diesel fuel exhibits the lowest mass fraction at the outlet, with a value of 0.13, whereas wood and coal exhibit values of 0.36 and 0.18, respectively. Combustion systems, such as internal combustion engines or gas turbines, exhibit fuel-rich regions within their respective combustion chambers where the fuel-air mixture is concentrated. In certain geographical areas, there may be insufficient oxygen to achieve full combustion, resulting in the occurrence of unreacted fuel in the exhaust [22].

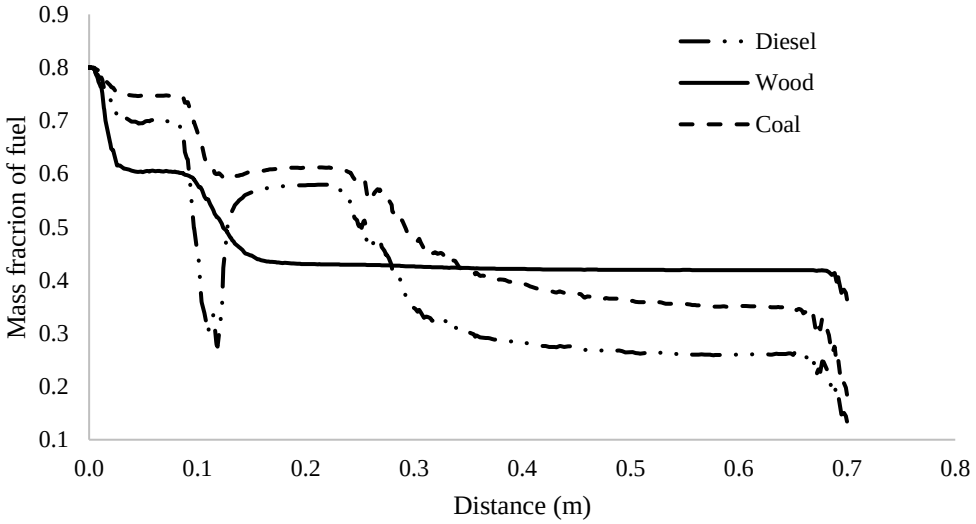

Figure 13: Mass fraction of fuel distribution at the middle line.

4.0 CONCLUSION

In conclusion, this study shows that the new combustion chamber design and performance of a Micro Gas Turbine (MGT) using Computational Fluid Dynamics (CFD) simulations provides a piece of knowledge for alternative fuels using wood. Wood-volatile-air fuel produces a stable outlet temperature of 1876.99 K, followed by coal and diesel. Wood has a pressure of 154 kPa and a similar pressure pattern to diesel and coal fuel. Wood gives the maximum burning velocity, 508.2 m/s, while diesel has the lowest. Wood-volatile-air has the lowest mass fraction of fuel at the outlet, 0.43 at 0.2 location and maintains higher compared to coal-hv-volatile and diesel have equivalent quantities. Even though diesel-air fuel has greater outlet temperatures and burning velocities, wood makes a significant contribution as the alternative fuel replacing the coal and diesel in the MGT chamber as a fuel.

ACKNOWLEDGMENT

The authors would like to acknowledge the financial support from the Ministry of Higher Education Malaysia under the Fundamental Research Grant Scheme (FRGS) (FRGS/1/2023/TK08/UTM/02/46) and Combustion Laboratory facilities in Universiti Teknologi Malaysia.

References

[1] Al-Attab, K. A., and Zainal, Z. A. (2014). Performance of a biomass-fuelled two-stage micro gas turbine (MGT) system with hot air production heat recovery unit. Applied Thermal Engineering, 70(1), 61–70. https://doi.org/10.1016/j.applthermaleng.2014.04.030

[2] Oppong, F., Van Der Spuy, J., Willem Von Backström, T., and Diaby, A. L. (n.d.). An overview of micro gas turbine engine performance investigation. Solar thermal treatment of manganese views project infrastructure for harvesting sustainable and renewable energy View project. https://doi.org/10.13140/RG.2.2.10055.09123

[3] Nascimento, M. A. R., Lora, E. S., Corrêa, P. S. P., Andrade, R. V., Rendon, M. A., Venturini, O. J., and Ramirez, G. A. S. (2008). Biodiesel fuel in diesel micro-turbine engines: Modelling and experimental evaluation. Energy, 33(2), 233–240. https://doi.org/10.1016/j.energy.2007.07.014

[4] Chiaramonti, D., Rizzo, A. M., Spadi, A., Prussi, M., Riccio, G., and Martelli, F. (2013). Exhaust emissions from liquid fuel micro gas turbine fed with diesel oil, biodiesel and vegetable oil. Applied Energy, 101, 349–356. https://doi.org/10.1016/j.apenergy.2012.01.066
[5] Enagi, I. I., Al-attab, K. A., and Zainal, Z. A. (2017). Combustion chamber design and performance for micro gas turbine application. Fuel Processing Technology, 166, 258–268. https://doi.org/10.1016/j.fuproc.2017.05.037
[6] Allen, C. A. W., Watts, K. C., Gunter, N., Scotia, C, Chris Watts, K., and Member, A. (2000). Comparative analysis of the atomization characteristics of fifteen biodiesel fuel types. 43(2), 207-211. https://doi.org/10.13031/2013.2695
[7] Black, F. (1991). An overview of the technical implications of methanol and ethanol as highway motor vehicle fuels. SAE Technical Paper 912413. International Fuels and Lubricants Meeting and Exposition Toronto, Canada. https://doi.org/10.4271/912413
[8] Laforgia, D., and Ardito, V. (1995). Biod1esel Fuelled IDI Engines: Performances, Emissions and Heat Release Investigation. Bioresource Technology, 51, 53-59.
[9] Mangra, A. C. (2020). Design and numerical analysis of a micro gas turbine combustion chamber. technology & applied science research, 10(6), 6422–6426. www.etasr.com
[10] Rabou, L. P. L. M., Grift, J. M., Conradie, R. E., and Fransen, S. (2008). Micro gas turbine operation with biomass producer gas and mixtures of biomass producer gas and natural gas. Energy and Fuels, 22(3), 1944–1948. https://doi.org/10.1021/ef700630z
[11] Magnussen & Hjertager
[12] Sann, E., Anwar, M., Adnan, R., & Idris, M. A. (2013). Biodiesel for Gas Turbine Application — An Atomization Characteristics Study. In Advances in Internal Combustion Engines and Fuel Technologies. InTech. https://doi.org/10.5772/54154
[13] Ofualagba, G. (2012). The modelling and simulation of a microturbine generation system. International Journal of Scientific and Engineering Research. 3 (2),267-274.
[14] Verhoeff, F., Rabou, L. P. L. M., Van Paasen, S. V. B., Emmen, F., Buwalda, R. A., Klein Teeselink, H. Proceedings of the 15th European Biomass Conference and Exhibition, Berlin, Germany; 2007; Contribution OA 7.5.
[15] Al-Halbouni, A., Giese, M., Flamme, K., Goerner, K. (2006). Applied modelling for bio- and lean gas fired micro gas turbines, Prog. Computational Fluid Dynamics, 6 (2006) 391–405.
[16] R. Calabria, F. Chiariello, P. Massoli, and F. Reale, "Numerical Study of a Micro Gas Turbine Fed by Liquid Fuels: Potentialities and Critical Issues," Energy Procedia, vol. 81, pp. 1131–1142, Dec. 2015, https://doi.org/10.1016/j.egypro.2015.12.138.
[17] John E. Matsson, An Introduction to ANSYS Fluent 2021 (2021).
[18] L. O. Rodrigues, H. S. Alencar, M. A. R. Nascimento, and O. J. Venturini, "Aerodynamic Analysis Using CFD for Gas Turbine Combustion Chamber," presented at the ASME 2007 Power Conference, Apr. 2009, https://doi.org/10.1115/POWER2007-22181.
[19] A. H. Lefebvre and Ballal, D. R. Gas Turbine Combustion: Alternative Fuels and Emissions, 3rd Edition. CRC Press, 2010.
[20] Lefebvre A. H. and McDonell, V. G., Atomization and Sprays, 2nd Edition. CRC Press, 2017.
[21] Fuchs, F., Meidinger, V., Neuburger, N., Reiter, T., Zündel, M., and Hupfer, A. (2016). "Challenges in designing very small jet engines – fuel distribution and atomization," in 16th International Symposium on Transport Phenomena and Dynamics of Rotating Machinery, Honolulu, HAW, April 2016.
[22] Prasetyo, E., Hermawan, R., Putra, A. L., and Zariatin, D. L. (2017). "Fluid flow analysis of micro gas turbine using computational fluid dynamics (CFD)," in Proceedings of the 4th IRSTC 2017, 2017.